CrystEngComm

www.rsc.org/crystengcomm

Volume 13 | Number 2 | 21 January 2011 | Pages 373–710

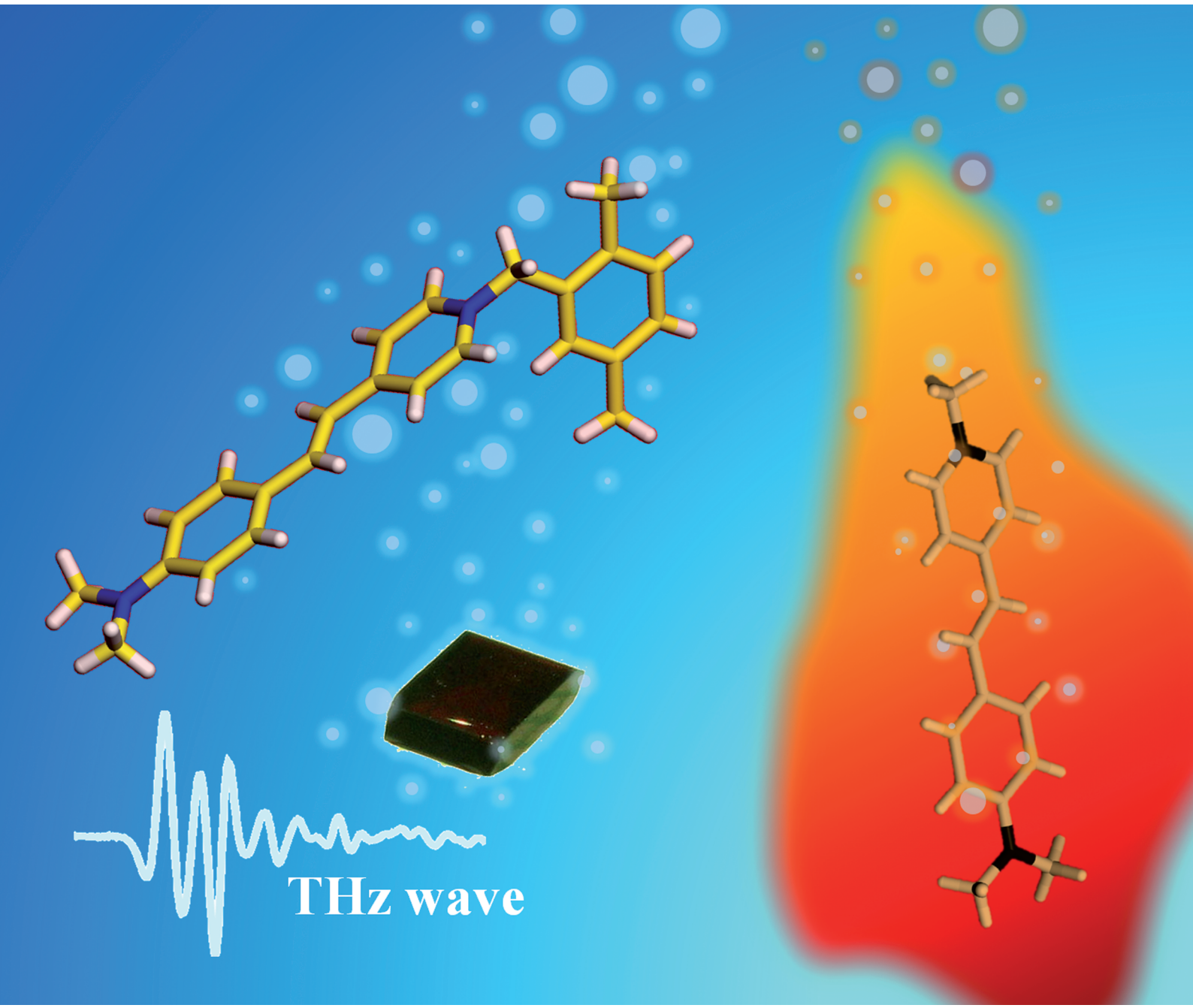

RSC Publishing

COVER ARTICLE

Kwon *et al.*

Acentric nonlinear optical *N*-benzyl stilbazolium crystals with high environmental stability and enhanced molecular nonlinearity in solid state

Acentric nonlinear optical *N*-benzyl stilbazolium crystals with high environmental stability and enhanced molecular nonlinearity in solid state†

Pil-Joo Kim,[a] Jae-Hyeok Jeong,[a] Mojca Jazbinsek,[b] Seong-Ji Kwon,[b] Hoseop Yun,[c] Jong-Taek Kim,[d] Yoon Sup Lee,[d] In-Hyung Baek,[c] Fabian Rotermund,[c] Peter Günter[b] and O-Pil Kwon*[a]

Received 27th July 2010, Accepted 2nd September 2010
DOI: 10.1039/c0ce00456a

We have developed a new cation core structure, *N*-benzyl stilbazolium nonlinear optical chromophore with a non-polar benzyl group to achieve acentric molecular ordering in the crystalline state. New *N*-benzyl stilbazolium crystal, BP3 (*N*,*N*-dimethylamino-*N*′-2,5-dimethylbenzyl-stilbazolium *p*-toluenesulfonate), exhibits an acentric crystal structure with the monoclinic $P2_1$ phase with a large macroscopic optical nonlinearity of 540 times the powder second harmonic generation efficiency of urea at the non-resonant wavelength of 1.9 μm. Compared to conventional rod-shaped *N*-alkyl stilbazolium crystals, an enhanced hyperpolarizability of the chromophores β_0 in the solid state can be utilized in bent-shaped *N*-benzyl stilbazolium crystals. This is attributed to the decreased inter-chromophore interactions due to the larger chromophore–chromophore separation induced by the bulky and bent-shaped *N*-benzyl group, so-called site-isolation effect. Moreover, by introducing the non-polar dimethylbenzyl group, BP3 crystals show a high environmental stability: they exhibit almost one order of magnitude smaller solubility in water than conventional stilbazolium crystals and also do not form a hydrated centrosymmetric phase even if crystallized in water-containing solvents. We have grown good optical quality crystals large enough for optical characterization. With as-grown BP3 crystals without additional polishing and cutting procedures we have demonstrated THz generation by optical rectification using 180 fs pulses at the pump wavelength of 836 nm.

Introduction

Organic nonlinear optical crystals[1] are very promising for numerous applications such as integrated photonics[2] and frequency conversion including THz wave generation.[3] Among organic crystals exhibiting the second-order (quadratic) optical nonlinearity, the benchmark materials are *N*-substituted stilbazolium crystals based on Coulomb interactions with large macroscopic optical nonlinearities.[4–8] Since DAST (*N*,*N*-dimethylamino-*N*′-methyl-stilbazolium *p*-toluenesulfonate) crystal based on *N*-methyl-stilbazolium cation has been first reported in 1989,[4a] many derivatives have been extensively investigated by using the same cation core structure, *N*-methyl-stilbazolium with various arylsulfonate anions:[5–7] for example, DSTMS with 2,4,6-trimethylbenzenesulfonate anion,[5] and DSNS with 2-naphthalenesulfonate anion.[6a] Another example of a core structure leading to the required acentric molecular ordering is *N*-aryl stilbazolium:[8] for example, DAPSH (*N*,*N*-dimethylamino-*N*′-phenyl-4-stilbazolium hexafluorophosphate) crystal with extremely large nonresonant macroscopic nonlinearity.[8b] In contrast to many studies with various counter anions, only few cation core structures that resulted in an acentric molecular ordering based on Coulomb interactions leading to large macroscopic nonlinearities have been reported, typically *N*-alkyl and *N*-aryl stilbazolium salts. Finding core structures for acentric molecular ordering in crystalline state is the starting point of crystal engineering, with the aim to obtain crystals with optimized optical and processing properties, as well as a high stability.

Although benchmark stilbazolium crystals exhibit a large macroscopic nonlinearity and good crystal characteristics, enhancing these physical properties including the environmental stability is a challenging topic. The salt-type stilbazolium chromophores are for example often dissolved in water and form a centrosymmetric hydrated phase in the presence of water,[9] and therefore humidity may damage the crystals, as well as limit the application of various crystal growth techniques. Also, the theoretical limits for the nonlinearities in stilbazolium salts have by far not been reached yet.[10] This is partially attributed to the decreased molecular nonlinearities in the solid state due to the interactions of the chromophores with the neighboring molecules.[10] For poled polymers it was shown that a bulky donor group and bulky isolation groups on the chromophore may help to decrease such interactions, *via* the so-called site-isolation effect,[11a] which is for polymer systems beneficial to achieve a higher poling efficiency and therefore a higher macroscopic nonlinearity.[11]

In this work, we develop new cation core structure, *N*-benzyl stilbazolium with a non-polar benzyl group for acentric molecular ordering in the crystalline system. New *N*-benzyl

[a]*Department of Molecular Science and Technology, Ajou University, Suwon, 443-749, Korea. E-mail: opilkwon@ajou.ac.kr; Fax: +82 31 219 1610; Tel: +82 31 219 2462*
[b]*Nonlinear Optics Laboratory, ETH Zurich, CH-8093 Zurich, Switzerland*
[c]*Division of Energy Systems Research, Ajou University, Suwon, 443-749, Korea*
[d]*Department of Chemistry and School of Molecular Science (BK 21), Korea Advanced Institute of Science and Technology (KAIST), Daejeon, 305-701, Korea*

† CCDC reference number 761254. For crystallographic data in CIF or other electronic format see DOI: 10.1039/c0ce00456a

stilbazolium crystal, BP3 (*N*,*N*-dimethylamino-*N*′-2,5-dimethylbenzyl-stilbazolium *p*-toluenesulfonate), exhibits an acentric crystal structure with the monoclinic $P2_1$ space group with a large macroscopic optical nonlinearity of 540 times the second harmonic generation efficiency as that of urea at the non-resonant wavelength of 1.9 μm. Compared to conventional rod-shaped *N*-alkyl stilbazolium crystals, an enhanced hyperpolarizability of the chromophores β_0 in the solid state is observed in bent-shaped *N*-benzyl stilbazolium crystals. Moreover, by introducing the non-polar dimethylbenzyl group, BP3 crystals show a high environmental stability: 9 times smaller solubility in water than the conventional stilbazolium crystal DAST. BP3 does not form a hydrated centrosymmetric phase even if crystallized in water-containing solvents. We have grown good optical quality crystals and have demonstrated THz generation by optical rectification of fs pulses with as-grown BP3 crystals without additional polishing and cutting procedures.

Results and discussion

Design of new core structure for acentric molecular ordering

The chemical structures of the new *N*-substituted stilbazolium derivatives are shown in Fig. 1. The chromophores consist of a *N*-substituted pyridinium electron acceptor group and the dimethylaminophenyl electron donor group. To induce asymmetry of the chromophores, which is one of the strategies to promote a noncentrosymmetric structure,[12] as well as achieve a site-isolation effect,[11] *N*-position on the pyridinium is substituted with a bent-shaped bulky benzyl group, replacing the methyl group of conventional rod-shaped *N*-alkyl stilbazolium DAST chromophores. Considering the environmental stability including water-insolubility, not only non-polar benzyl group, but also non-polar methyl groups on the benzyl ring are introduced for BP2 and BP3. In order to maintain the main supramolecular Coulomb interactions of these compounds, we use non-polar substituents such as benzyl and methyl groups, which may form only weak intermolecular interactions. This is because polar substituents on the benzyl ring may form unexpected additional strong intermolecular interactions such as hydrogen bonds and dipole–ion interactions, which may diminish the hyperpolarizability of the molecules in the solid state.[10,11,13] In BP3 chromophore, the *ortho* and the *meta* positions of the two methyl groups on the benzyl ring are expected to increase the asymmetry of the chromophore shape.

The chromophores were synthesized by metathesization of corresponding *N*,*N*-dimethylamino-*N*′-benzylstilbazolium chloride salt with *p*-toluenesulfonate sodium salt in water.[5,6] First, the corresponding *N*-benzylpicolinium chloride derivatives were prepared by the reaction of picoline with appropriated chlorobenzyl derivatives. *N*,*N*-Dimethylamino-*N*′-benzylstilbazolium chloride salts were synthesized by a condensation of *N*-benzylpicolinium chloride with dimethylaminobenzaldehyde. The BP chromophores synthesized in water were recrystallized in methanol by the rapid cooling method for purification and removing residual water.

Basic characterization of *N*-benzyl stilbazolium molecules and crystals

Fig. 2 shows the absorption spectra of the *N*-benzyl stilbazolium BP chromophores in methanol. The wavelength of maximum absorption of the investigated BP chromophores is $\lambda_{max} \approx 487$ nm, which is about 12 nm higher than for the *N*-methyl stilbazolium chromophores (for example, DAST $\lambda_{max} = 475$ nm).[4] According to the well-known nonlinearity-transparency trade-off;[1] *N*-substituted stilbazolium chromophores with a higher molecular nonlinearity generally exhibit a red shift of λ_{max}.[8c] *N*-Benzyl BP chromophores are therefore expected to exhibit a higher molecular nonlinearity than *N*-alkyl stilbazolium chromophores.

In order to investigate the molecular nonlinearity of the new *N*-benzyl stilbazolium derivatives in more details, we calculated the first hyperpolarizability tensor β_{ijk} and the maximal first hyperpolarizability β_{max} (hyperpolarizability component along the main charge-transfer direction) of the cation core structures of DAST and BP3 crystals by quantum chemical calculations[14] using the hybrid functional B3LYP[15] with the 6-311 + G(d) basis set. The optimized structures (OPTs) obtained by using the density functional theory (DFT) of the cations, *N*,*N*-dimethylamino-*N*′-methyl-stilbazolium for DAST and *N*,*N*-dimethylamino-*N*′-2,5-dimethylbenzyl-stilbazolium for BP3 are shown in Fig. 3 and the calculated results are listed in Table 1. The calculated molecular hyperpolarizability of the *N*-benzyl BP3 cation is about 22% higher than that of the *N*-methyl DAST

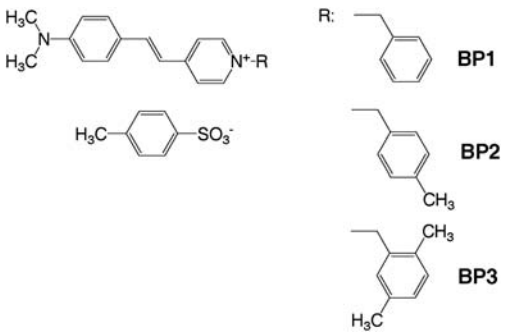

Fig. 1 Chemical structures of *N*-benzyl pyridinium salt derivatives and their abbreviations.

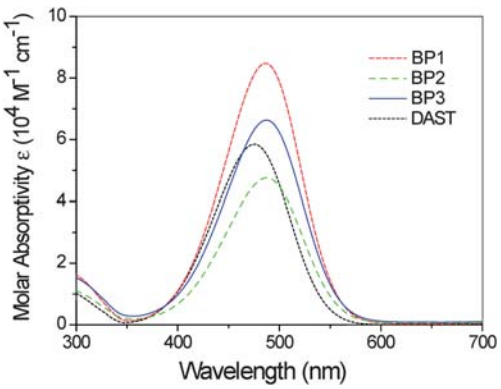

Fig. 2 Absorption spectra of salt molecules in methanol solution: $\lambda_{max} =$ 475 nm for DAST and ~ 487 nm for BP chromophores.

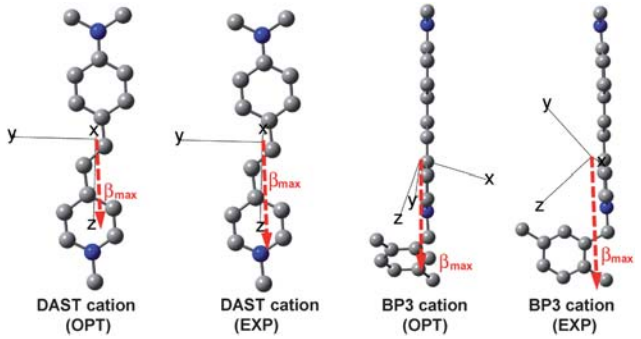

Fig. 3 Representation of the optimized cation structures (OPTs) obtained by the density functional theory (DFT) using B3LYP/6-311 + G(d) and the experimental cation structures (EXPs) obtained by the X-ray diffraction of acentric single crystals of DAST (*N*,*N*-dimethylamino-*N*′-methyl-stilbazolium *p*-toluenesulfonate) and BP3 (*N*,*N*-dimethylamino-*N*′-2,5-dimethylbenzyl-stilbazolium *p*-toluenesulfonate). The dotted vectors present the directions of the maximum first hyperpolarizability β_{max} of the cations as determined by finite-field calculations (see Table 1).

Table 1 Calculated results of the finite-field (FF) method with the optimized (OPT) and the experimental (EXP) cation structures of DAST and BP3 crystals at B3LYP/6-311 + G(d) level: the zero-frequency hyperpolarizability tensor β_{ijk} ($\times 10^{-30}$ esu) and the maximum first hyperpolarizability β_{max} ($\times 10^{-30}$ esu)

	DAST cation (OPT)	DAST cation (EXP)	BP3 cation (OPT)	BP3 cation (EXP)
β_{xxx}	−0.11	−0.21	3.73	0.61
β_{xxy}	−0.04	0.03	8.12	2.85
β_{xyy}	0.05	−0.05	16.29	−2.27
β_{yyy}	−0.42	−0.06	30.26	−96.43
β_{xxz}	0.18	0.25	10.37	−2.57
β_{xyz}	0.00	0.38	23.69	2.40
β_{yyz}	−4.85	−3.89	49.22	86.30
β_{xzz}	0.38	−1.28	30.58	−2.16
β_{yzz}	−2.59	−3.86	69.87	−76.69
β_{zzz}	158.76	193.60	85.59	65.81
β_{max}	159.05	193.85	194.06	231.78

cation, which shows a good agreement with the measured wavelength of maximum absorption as discussed above.

The melting temperature of the chromophores was determined by the differential scanning calorimetry (DSC). The BP crystals having more methyl groups exhibit a higher melting temperature: 210 °C for BP1 with benzyl group, 225 °C for BP2 with methylbenzyl group, and 250 °C for BP3 with dimethylbenzyl group.

To investigate the macroscopic non-resonant optical nonlinearity we performed the Kurtz and Perry second harmonic generation (SHG) powder test at the fundamental wavelength of 1.9 μm.[16] The second harmonic generation signals of BP crystalline powders were compared to that of DAST. The BP3 crystals exhibited a large SHG signal of about 54% as that of DAST or 540 times as that of urea, while for BP1 and BP2 crystals the SHG signal was absent. From this result we may expect a noncentrosymmetric crystal structure for BP3 crystals with well-aligned chromophores, leading to a large macroscopic nonlinearity. BP3 crystals are therefore very attractive materials for second-order nonlinear optical applications.

Single crystal structure and nonlinear optical properties

Single BP3 crystals for crystal structure analysis by X-ray diffraction (XRD) were grown from methanol solution by slow evaporation method at 40 °C in an oven. The BP3 crystals have an acentric monoclinic crystal structure with $P2_1$ space group (point group 2). Its molecular structure and the crystal packing are shown in Fig. 4 and 5. While the *N*-alkyl and *N*-aryl stilbazolium part including the dimethylamino group presents a rod-shape in previously investigated stilbazolium salts,[4–8] *N*-substituted benzyl group is out of the plane of the stilbazolium and the BP3 cation possesses a non-rod-shape (see Fig. 4a), which can induce asymmetry and a different kind of acentric molecular ordering.

In *N*-alkyl DAST, where the same counter anion is used, as well as in other DAST derivatives with a different counter anion and a non-centrosymmetric structure, well defined polar sheets of stilbazolium chromophores and counter anions can be identified in the crystal structure.[4a,6b] In BP3, no such layers are observed, which means that the *N*-benzyl stilbazolium substitution essentially changes the characteristic packing tendency of DAST derivatives. Main supramolecular interactions of acentric BP3 crystal are Coulomb interaction between cations and anions and hydrogen bonds with S–O···H–C (see Fig. 5). However, as shown in Fig. 3, the main charge transfer character is still essentially one-dimensional and the main charge-transfer

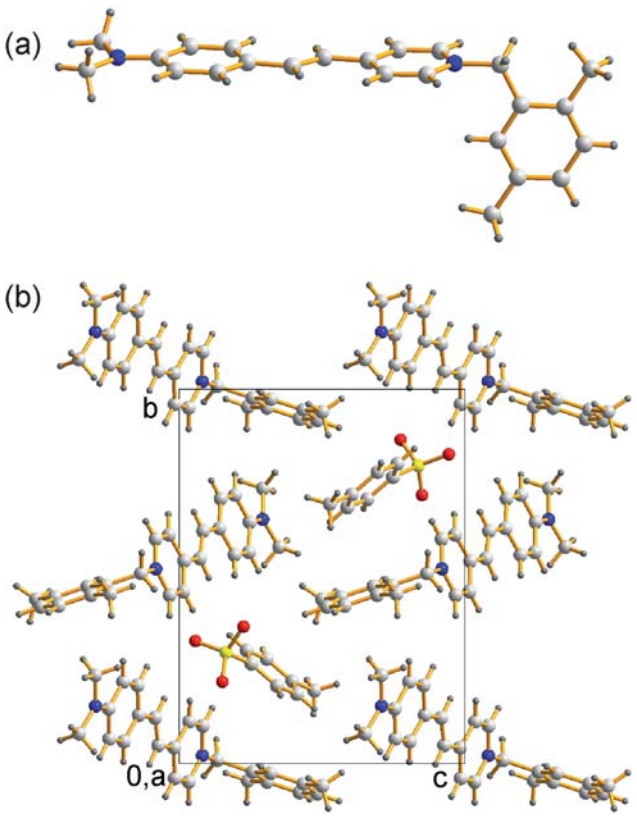

Fig. 4 (a) Molecular structure of the acentric cation core of the BP3 chromophore as determined by the X-ray crystallography. (b) Crystal packing diagram projected along the *a*-axis for the monoclinic BP3 crystals. The polar 2-fold axis is along the *b* crystallographic axis.

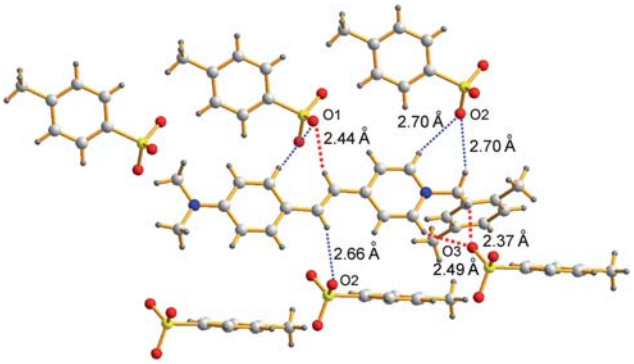

Fig. 5 Supramolecular interactions of BP3 crystals: hydrogen-bond interactions with a O···H–C distance of below 2.5 Å and 2.6–2.8 Å are illustrated by thick and thin dotted lines, respectively.

direction (along β_{max} in Fig. 3) in the non-rod-shaped *N*-benzyl BP3 is still along the long axis of the stilbazolium core like it is in DAST derivatives.

The main charge transfer direction of the chromophores makes an angle of about $\theta = 79°$ with respect to the polar axis *b* of the BP3 crystals. This means that the order parameter $\cos^3\theta$ of BP3 is considerably reduced compared to DAST with $\theta = 20°$. We can estimate the relative powder SHG test efficiency of both crystals by comparing the theoretical figure of merit $N^2\langle(\beta^{eff})^2\rangle$, where *N* is the number density of the chromophores and the squared effective hyperpolarizability β, averaged over all possible orientations.[16] We calculated the effective first-hyperpolarizability components β_{ijk}^{eff} in the crystal by considering the orientation of the chromophores in the solid state; the results are listed in the Table 2. For DAST, because of the high order parameter, the maximum component of β_{ijk}^{eff} is diagonal, $\beta_{111}^{eff} = 161 \times 10^{-30}$ esu, the largest off-diagonal component is $\beta_{221}^{eff} = 21 \times 10^{-30}$ esu, while all other components are considerably smaller. On the other hand, for BP3 the off-diagonal component is the largest $\beta_{112}^{eff} = 45 \times 10^{-30}$ esu, while the diagonal component is very small $\beta_{222}^{eff} \approx 1 \times 10^{-30}$ esu. We can use these results to estimate the average as described in ref. 16. Assuming the calculated first-hyperpolarizability values in the gas phase and their projections in the crystal structure for BP3 and DAST, the parameter $N^2\langle(\beta^{eff})^2\rangle$ for BP3 is only about 10% of the one for DAST, $N^2\langle(\beta^{eff})^2\rangle \cong 2000 \times 10^{-60}$ esu^2 m^{-3} for BP3 and $N^2\langle(\beta^{eff})^2\rangle \cong 19\,000 \times 10^{-60}$ esu^2 m^{-3} for DAST. This cannot explain the observed powder SHG test efficiency of BP3 crystals, which is more than five times higher compared to the expected one (*i.e.* 54% of DAST). One possible reason is a relatively bulky and bent-shaped group at the end of the chromophore, which considerably reduces the number density of the BP3 chromophores in the crystalline state, by more than 20% compared to DAST. Due to the decreased inter-chromophore interactions in the crystalline system by the site-isolation effect,[11a] this may be beneficial for enhancing (or not reducing) the hyperpolarizability of the chromophores β_0 in the solid state. Indeed, for DAST it was shown that the hyperpolarizabilities in the solid state are reduced by more than 80% compared to solution because of intermolecular interactions.[10] We can therefore expect even much higher macroscopic second-order nonlinearities if BP3 chromophores can be packed in a more optimal way by using for example other counter anions.

Table 2 The components of the non-resonant effective hyperpolarizability tensor ($\times 10^{-30}$ esu) in the Cartesian system (x_1,x_2,x_3) rotated by an angle of 1° and 26° for DAST and BP3, respectively, from the crystallographic *a*-axis toward the *c*-axis around the symmetry x_2 = *b*-axis, considering the X-ray crystal structure and the β_{ijk} components calculated for the EXP molecular structures (see Table 1)

	β_{111}^{eff}	β_{221}^{eff}	β_{331}^{eff}	β_{113}^{eff}	β_{223}^{eff}	β_{333}^{eff}
DAST	161	21	−3.2	0	1.0	−0.3
	β_{112}^{eff}		β_{222}^{eff}	β_{332}^{eff}		β_{123}^{eff}
BP3	45		0.8	0.5		0

Environmental stability and bulk crystal growth

Environmental stability of water-soluble stilbazolium derivatives studied previously exhibits some limits for practical applications. In order to investigate the humidity resistance, the solubility of BP3 crystals in water was measured. BP3 crystals exhibit 9 times lower solubility (0.022 mmol per 100 g water) in water at 30 °C than DAST crystals (0.20 mmol per 100 g water). The reduced solubility in water is attributed to introducing the non-polar *N*-benzyl groups with two methyl substituents.

Many examples of stilbazolium derivatives form a hydrated phase with water.[9] DAST crystals form a hydrated phase with a centrosymmetric structure.[9a] In order to examine the tendency of forming hydrated phases, BP3 and DAST crystals were crystallized in water-containing solvents. BP3 and DAST crystals were recrystallized by rapid cooling method in methanol/water (1 : 1 and 1 : 2 v/v) and subsequently powder X-ray diffraction and differential scanning calorimetry were measured. In all experiments, BP3 crystals did not form any hydrated phase or other polymorphs showing a practically identical X-ray diffraction pattern (see Fig. 6) and thermodiagram (not shown), while DAST crystals formed the centrosymmetric hydrated phase in the presence of water. This high environmental stability with low water-solubility without hydrated polymorphs is an advantage

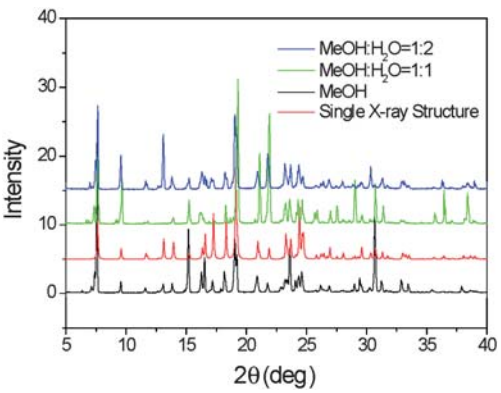

Fig. 6 Powder X-ray diffraction patterns of BP3 crystals crystallized in various solvents including those containing water.

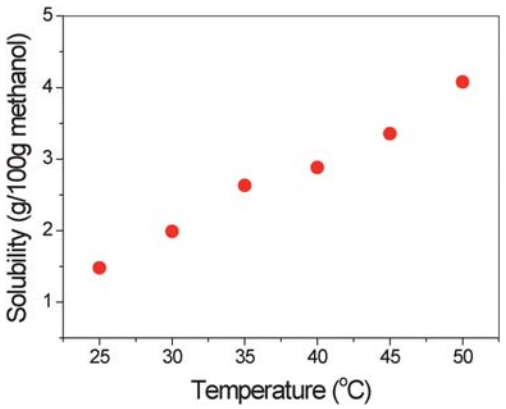

Fig. 7 Solubility as a function of temperature for BP3 in methanol.

for some practical applications and also for applying various crystal growth techniques.

While having an extremely low solubility in water, BP3 crystals exhibit a solubility in methanol high enough for bulk crystal growth. Fig. 7 shows the solubility in methanol for BP3 crystals, which is in the same order of magnitude as for DAST crystals (2.9 g BP3 per 100 g methanol compared to 3.7 g DAST/100 g methanol at 40 °C). Since the hydrated phase does not form, we can grow BP3 crystals not only by the slow cooling method, but also by the slow evaporation method. Bulk DAST crystals cannot be easily grown by the slow evaporation method because of the easy formation of the hydrated phase. BP3 crystals grown by the slow evaporation method exhibit the identical crystal structure as those grown by the rapid cooling method in the powder XRD experiments.

Examples of the as-grown bulk BP3 crystals grown by the slow cooling method and the slow evaporation method are shown in Fig. 8a and b. The growth of good quality crystals with side lengths of up to 4 mm is relatively easy even without optimizing the temperature gradients or evaporation rates, in contrast *e.g.* to other stilbazolium derivatives such as *N*-aryl stilbazolium derivatives,[17] and relatively large size crystals can be grown by both slow cooling and slow evaporation.

The X-ray diffraction shows that the large surface of the crystals is the (001) face. As-grown BP3 crystals exhibit a good optical quality, as well as nice and flat surfaces. Fig. 8c shows the transmission spectra with polarized light of an un-polished as-grown BP3 crystal for light polarization parallel and perpendicular to the polar *b*-axis as presented in Fig. 8b. The crystal is transparent between 800 nm and 2100 nm with a small absorption band at about 1700 nm, which is most probably due to the overtones of the C–H stretching vibrations. We obtained a relatively good transmission in the transparent region. This shows that the quality and parallelism of the crystal surfaces are quite good even without polishing or cutting these as-grown samples.

THz generation

We demonstrate THz pulse generation in an as-grown unpolished 560 μm thick BP3 crystal using a 1 kHz repetition rate Ti:Sapphire regenerative amplifier (Coherent Inc., Legend) as the pump source, delivering 180 fs pulses at 836 nm. The output beam from the amplifier was divided into the pump and the probe beam for the generation and the detection of THz pulses, respectively.[18] Single pulse energies of up to 380 μJ were used for

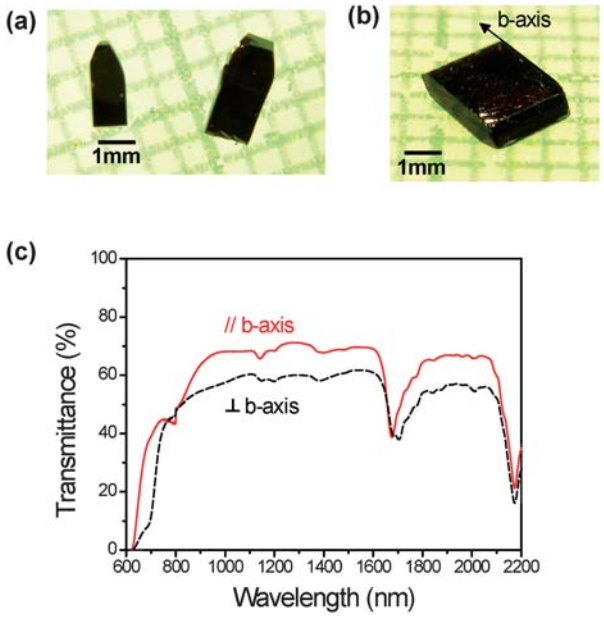

Fig. 8 BP3 bulk crystals grown by (a) the slow cooling method with the cooling rate of 1 °C per day from 40 °C and (b) the slow evaporation method at 40 °C. The large surface is the (001) face. (c) Transmission spectra of an unpolished 560 μm thick BP3 crystals (b) grown by the slow evaporation method. The light was incident normal to the (001) as-grown face with polarization parallel or perpendicular to the polar *b*-axis.

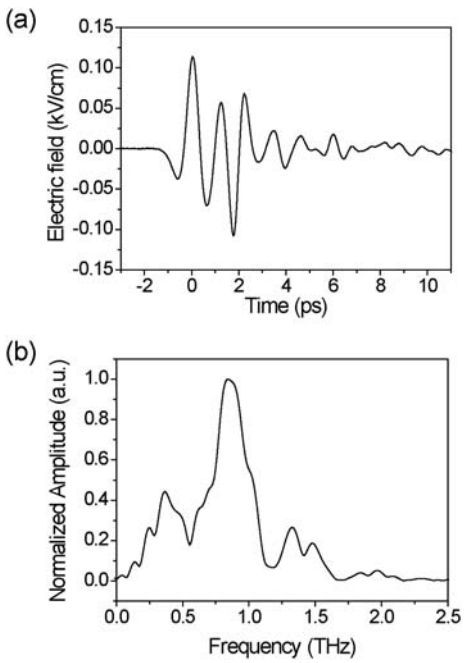

Fig. 9 THz pulse generated in a 560 μm thick BP3 crystal using 180 fs pump pulses with the pulse energy of 380 μJ and repetition rate of 1 kHz at 836 nm. (a) Time trace of the generated THz electric field and (b) the corresponding spectrum.

the THz pulse generation by optical rectification. The pump polarization was close to the *a*-axis for the effective use of the largest off-diagonal nonlinear optical susceptibility component $\chi^{(2)}_{211}$. After the generation of the THz waves in the BP3 crystal, the pump pulses were filtered out by using a Si wafer. The generated THz pulses were subsequently collimated and focused into the ZnTe detection crystal by using a telescope and off-axis parabolic mirrors. The electric field of the generated THz pulses was measured in a 1 mm thick ⟨110⟩ ZnTe crystal by electro-optic sampling technique, where the detection crystal was rotated around the propagation direction to obtain the maximum THz signal. All the measurements were performed at room temperature.

Fig. 9a shows the time trace of the THz electric field generated in the BP3 crystal. Quasi-single cycle and sub-ps THz pulses were successfully generated with 836 nm pumping. This wavelength corresponds to the operation wavelength of widely spread femtosecond laser amplifiers. The spectrum of the generated THz pulses is shown in Fig. 9b. The center frequency of the spectrum was 0.84 THz. Note that the two stronger absorption bands appeared at around 0.6 and 1.2 THz, which are attributed partially to ambient water vapor as well as optical phonon resonance in BP3 material, similar as observed in DAST at 1.1 THz.

Conclusions

We have developed a new cation core structure, *N*-benzyl stilbazolium nonlinear optical chromophore with a non-polar benzyl group to achieve acentric molecular ordering in the crystalline state. New *N*-benzyl stilbazolium crystal, BP3 (*N*,*N*-dimethylamino-*N*′-benzylstilbazolium *p*-toluenesulfonate), exhibits an acentric crystal structure with monoclinic $P2_1$ phase with a large macroscopic optical nonlinearity of 540 times larger second harmonic generation efficiency than in urea at a non-resonant wavelength of 1.9 μm. Compared to the conventional rod-shaped *N*-alkyl stilbazolium, an enhanced hyperpolarizability of the chromophores β_0 in the solid state can be utilized in bent-shaped *N*-benzyl stilbazolium crystals. This is attributed to the decreased inter-chromophore interactions due to the larger chromophore–chromophore separation (*i.e.*, site-isolation effect) induced by the bulky and bent-shaped *N*-benzyl group. Moreover, by introducing the non-polar dimethylbenzyl group, BP3 crystals show a high environmental stability: they possess 9 times smaller solubility in water than conventional stilbazolium crystals and at the same time do not form a hydrated centrosymmetric phase even if crystallized in water-containing solvents. We have successfully demonstrated THz generation with as-grown BP3 crystals without performing any polishing and cutting procedures by optical rectification using 180 fs pulses at the pump wavelength of 836 nm. Therefore, new cation core structure, *N*-benzyl stilbazolium crystals are very promising materials for second-order nonlinear optical applications.

Experimental

Synthesis

All chemicals were purchased from commercial suppliers, mainly from Aldrich, and used without further purification. ^{1}H-NMR data were recorded on a Varian 400 MHz. All chemical shifts are reported in ppm (δ) relative to $(CH_3)_4Si$. The products were prepared by the following synthetic routes and dried during 2 hours at 60 °C in a vacuum oven prior to characterization.

Synthesis of BP*n*Cl. For BP3Cl, 2,5-dimethylbenzyl chloride (0.1556 mol, 15.25 ml) and 4-picoline (0.1556 mol, 23 ml) were dissolved in acetonitirile (150 ml) and the mixture was stirred for 2 days at 70 °C. The resulting mixture was cooled to room temperature. After cooling, the precipitate was filtered off and then washed with diethyl ether. White-pink solid product was obtained and dried in vacuum oven to remove solvent. The solid product (0.137 mol, 34 g) and 4-dimethyl aminobenzaldehyde (0.137 mol, 20.5 g) were dissolved in methanol (300 ml). The solution was completely dissolved with catalyst piperidine (0.0274 mol, 2.7 ml). The resulting solution was stirred under reflux for 24 h at 80 °C and cooled to room temperature. After adding ethanol and diethyl ether, black purple precipitate was filtered off and washed with diethyl ether. For BP1 and BP2, an analogous procedure was employed by using the corresponding starting materials, benzyl chloride for BP1Cl and 4-methylbenzyl chloride for BP2Cl.

N,N-*Dimethylamino*-N′-*benzyl-stilbazolium chloride (BP1Cl).* Yield = 63%, ^{1}H-NMR (400 MHz, CD_3OD): δ = 8.61 (d, 2H, J = 7.2 Hz, C_5H_4N), 7.96 (d, 2H, J = 6.8 Hz, C_5H_4N), 7.84 (d, 1H, J = 16.0 Hz, CH), 7.60 (d, 2H, J = 8.8 Hz, C_6H_4), 7.45 (m, 5H, C_6H_5), 7.08 (d, 1H, J = 15.6 Hz, CH), 6.78 (d, 2H, J = 8.8 Hz, C_6H_4), 5.62 (s, 2H, CH_2), 3.07 (s, 6H, NMe).

N,N-*Dimethylamino*-N′-*4-methylbenzyl-stilbazolium chloride (BP2Cl).* Yield = 51%, ^{1}H-NMR (400 MHz, CD_3OD): δ = 8.59 (d, 2H, J = 6.8 Hz, C_5H_4N), 7.95 (d, 2H, J = 7.2 Hz, C_5H_4N), 7.82 (d, 1H, J = 16.4 Hz, CH), 7.59 (d, 2H, J = 8.8 Hz, C_6H_4), 7.34 (d, 2H, J = 8.0 Hz, $C_6H_4CH_3$), 7.27 (d, 2H, J = 7.6 Hz, $C_6H_4CH_3$), 7.07 (d, 1H, J = 15.6 Hz, CH), 6.77 (d, 2H, J = 9.2 Hz, C_6H_4), 5.56 (s, 2H, CH_2), 3.07 (s, 6H, NMe), 2.36 (s, 3H, Me).

N,N-*Dimethylamino*-N′-*2,5-dimethylbenzyl-stilbazolium chloride (BP3Cl).* Yield = 43%, ^{1}H-NMR (400 MHz, CD_3OD): δ = 8.48 (d, 2H, J = 6.8 Hz, C_5H_4N), 7.95 (d, 2H, J = 6.8 Hz, C_5H_4N), 7.84 (d, 1H, J = 16.4 Hz, CH), 7.60 (d, 2H, J = 9.2 Hz, C_6H_4), 7.19 (s, 2H, $C_6H_3Me_2$), 7.10 (s, 1H, $C_6H_3Me_2$), 7.08 (d, 1H, J = 16.4 Hz, CH), 6.78 (d, 2H, J = 8.8, C_6H_4), 5.63 (s, 2H, CH_2), 3.07 (s, 6H, NMe), 2.34 (s, 3H, Me), 2.27 (s, 3H, Me).

Synthesis of chromophore BP*n*. For example of BP3, BP3Cl (2.64 mmol, 1 g) was completely dissolved in boiling water (100 ml). The *p*-toluenesulfonic acid sodium salt (7.92 mmol, 1.54 g) was dissolved in water (10 ml) and dropwise added into the solution of BP3Cl. The solution was cooled to room temperature and precipitate is filtered off and washed with water. The filtrate was dried for 1 h at 100 °C in vacuum oven. The final product was obtained by recrystallization in methanol.

N,N-*Dimethylamino*-N′-*benzyl-stilbazolium* p-*toluenesulfonate (BP1).* Yield = 53%, ^{1}H-NMR (400 MHz, CD_3OD): δ = 8.60 (d, 2H, J = 7.2 Hz, C_5H_4N), 7.95 (d, 2H, J = 6.8 Hz, C_5H_4N), 7.83

(d, 1H, $J = 16.4$ Hz, CH), 7.69 (d, 2H, $J = 8.0$, $C_6H_4SO_3^-$), 7.59 (d, 2H, $J = 8.8$ Hz, C_6H_4), 7.45 (m, 5H, C_6H_5), 7.21 (d, 2H, $J = 8.4$ Hz, C_6H_4), 7.07 (d, 1H, $J = 16.0$ Hz, CH), 6.77 (d, 2H, $J = 8.8$ Hz, C_6H_4), 5.61 (s, 2H, CH_2), 3.07 (s, 6H, NMe), 2.36 (s, 3H, Me). Elemental analysis for $C_{29}H_{30}N_2O_3S$: (%) calcd C 71.58, H 6.21, N 5.76, S 6.59; found: C 71.50, H 6.45, N 5.48, S 6.06%.

N,N-*Dimethylamino*-N′-*4-methylbenzyl-stilbazolium* p-*toluenesulfonate (BP2)*. Yield = 77%, ^{1}H-NMR (400 MHz, CD_3OD): $\delta = 8.56$ (d, 2H, $J = 6.8$ Hz, C_5H_4N), 7.94 (d, 2H, $J = 7.2$ Hz, C_5H_4N), 7.82 (d, 1H, $J = 16.0$ Hz, CH), 7.69 (d, 2H, $J = 8.0$, $C_6H_4SO_3^-$), 7.59 (d, 2H, $J = 9.2$ Hz, C_6H_4), 7.34 (d, 2H, $J = 8.0$, $C_6H_4CH_3$), 7.27 (d, 2H, $J = 8.0$ Hz, $C_6H_4CH_3$), 7.21 (d, 2H, $J = 8.4$ Hz, $C_6H_4SO_3^-$), 7.06 (d, 1H, $J = 16.0$ Hz, CH), 6.77 (d, 2H, $J = 8.8$, C_6H_4), 5.55 (s, 2H, CH_2), 3.07 (s, 6H, NMe), 2.36 (s, 6H, Me). Elemental analysis for $C_{30}H_{32}N_2O_3S$: (%) calcd C 71.97, H 6.44, N 5.60, S 6.40; found: C 71.94, H 6.43, N 5.56, S 6.43%.

N,N-*Dimethylamino*-N′-*2,5-dimethylbenzyl-stilbazolium* p-*toluenesulfonate (BP3)*. Yield = 70%, ^{1}H-NMR (400 MHz, CD_3OD): $\delta = 8.46$ (d, 2H, $J = 6.8$ Hz, C_5H_4N), 7.94 (d, 2H, $J = 6.8$ Hz, C_5H_4N), 7.83 (d, 1H, $J = 16.0$ Hz, CH), 7.69 (d, 2H, $J = 8.4$, $C_6H_4SO_3^-$), 7.59 (d, 2H, $J = 8.8$ Hz, C_6H_4), 7.20 (d, 2H, $J = 8.8$, $C_6H_4SO_3^-$), 7.19 (s, 2H, $C_6H_3Me_2$), 7.10 (s, 1H, $C_6H_3Me_2$), 7.07 (d, 1H, $J = 16.4$ Hz, CH), 6.77 (d, 2H, $J = 8.8$ Hz, C_6H_4), 5.62 (s, 2H, CH_2), 3.07 (s, 6H, NMe), 2.36 (s, 3H, Me), 2.34 (s, 3H, Me), 2.26 (s, 3H, Me). Elemental analysis for $C_{31}H_{34}N_2O_3S$: (%) calcd C 72.34, H 6.66, N 5.44, S 6.23; found: C 72.36, H 6.69, N 5.44, S 6.21%.

Powder SHG test

The crystalline powder was grinded and prepared in a quartz cell of 1 mm thickness. The laser pulses at the wavelength 1907 nm were generated by focusing Q-switched Nd:YAG nanosecond laser pulses ($\lambda = 1064$ nm, repetition rate 10 Hz) into a high-pressure Raman cell filled with H_2. The fundamental beam was removed by appropriate filters. The transmitted second-harmonic signal at 953.5 nm was detected by a photomultiplier and averaged over several laser pulses. The measurements were performed on a parallel sample and the measured intensities of the second-harmonic signal were averaged over several sample positions.

X-Ray crystal structure analysis

Crystal structure data for BP3: $C_{31}H_{34}N_2O_3S$, $M_r = 514.66$, monoclinic, space group $P2_1$, $a = 7.6688(3)$ Å, $b = 15.1880(6)$ Å, $c = 11.8332(5)$ Å, $\beta = 101.347(1)°$, $V = 1351.32(9)$ Å^3, $Z = 2$, $T = 290(1)$ K, crystal dimension $0.45 \times 0.40 \times 0.10$ mm^3, $\mu(MoK_\alpha) = 0.155$ mm^{-1}. Of 10 620 reflections collected in the θ range 3.0°–25.0° using an ω scans on a Rigaku *R*-axis Rapid S diffractometer, 4726 were unique reflections ($R_{int} = 0.029$, completeness = 99.8%). The structure was solved and refined against F^2 using SHELX97,[19] 335 variables, w$R_2 = 0.0969$, $R_1 = 0.0337$ ($F_o^2 > 2\sigma(F_o^2)$), GOF = 1.094, Flack parameter $x = -0.05(7)$, and max/min residual electron density 0.182/−0.178 e Å^{-3}.

Acknowledgements

This work has been supported by the National Research Foundation of Korea Grant (NRF) funded by the Korea government (MEST) (No. 2009-0084918), Priority Research Centers Program through the National Research Foundation of Korea (NRF) funded by the Ministry of Education, Science and Technology (2010-0028294), and by the Swiss National Science Foundation.

References

1 (*a*) Ch. Bosshard, M. Bösch, I. Liakatas, M. Jäger and P. Günter, in *Nonlinear Optical Effects and Materials*, ed. P. Günter, Springer-Verlag, Berlin, 2000, ch. 3; (*b*) Ch. Bosshard, K. Sutter, Ph. Prêtre, J. Hulliger, M. Flörsheimer, P. Kaatz and P. Günter, in *Organic Nonlinear Optical Materials; Advances in Nonlinear Optics*, Gordon and Breach Science Publishers, Langhorne, PA, 1995, vol. 1; (*c*) H. S. Nalwa, T. Watanabe and S. Miyata, in *Nonlinear Optics of Organic Molecules and Polymers*, ed. H. S. Nalwa and S. Miyata, CRC Press, 1997, ch. 4; (*d*) D. S. Chemla and J. Zyss, in *Nonlinear Optical Properties of Organic Molecules and Crystals*, Academic Press, 1987, vol. 1.

2 (*a*) M. Jazbinsek, O. P. Kwon, Ch. Bosshard and P. Günter, in *Handbook of Organic Electronics and Photonics*, ed. S. H. Nalwa, American Scientifirc Publishers, Los Angeles, 2008, ch. 1; (*b*) L. Dalton, P. Sullivan and A. K. Y. Jen, in *Handbook of Photonics*, ed. M. C. Gupta and J. Ballato, CRC Press, Boca Raton, FL, 2007; (*c*) H. Figi, M. Jazbinsek, Ch. Hunziker, M. Koechlin and P. Günter, *Opt. Express*, 2008, **16**, 11310; (*d*) T. Kaino, B. Cai and K. Takayama, *Adv. Funct. Mater.*, 2002, **12**, 599.

3 (*a*) O. P. Kwon, S. J. Kwon, M. Jazbinsek, F. D. J. Brunner, J. I. Seo, Ch. Hunziker, A. Schneider, H. Yun, Y. S. Lee and P. Günter, *Adv. Funct. Mater.*, 2008, **18**, 3242; (*b*) M. Tonouchi, *Nat. Photonics*, 2007, **1**, 97; (*c*) B. Ferguson and X. C. Zhang, *Nat. Mater.*, 2002, **1**, 26; (*d*) H. Hashimoto, H. Takahashi, T. Yamada, K. Kuroyanagi and T. Kobayashi, *J. Phys.: Condens. Matter*, 2001, **13**, L529.

4 (*a*) S. R. Marder, J. W. Perry and W. P. Schaefer, *Science*, 1989, **245**, 626; (*b*) S. R. Marder, J. W. Perry and C. P. Yakymyshyn, *Chem. Mater.*, 1994, **6**, 1137; (*c*) F. Pan, G. Knöpfle, Ch. Bosshard, S. Follonier, R. Spreiter, M. S. Wong and P. Günter, *Appl. Phys. Lett.*, 1996, **69**, 13.

5 (*a*) Z. Yang, L. Mutter, M. Stillhart, B. Ruiz, S. Aravazhi, M. Jazbinsek, A. Schneider, V. Gramlich and P. Günter, *Adv. Funct. Mater.*, 2007, **17**, 2018; (*b*) L. Mutter, F. D. J. Brunner, Z. Yang, M. Jazbinsek and P. Günter, *J. Opt. Soc. Am. B*, 2007, **24**, 2556; (*c*) M. Stillhart, A. Schneider and P. Günter, *J. Opt. Soc. Am. B*, 2008, **25**, 1914.

6 (*a*) B. Ruiz, Z. Yang, V. Gramlich, M. Jazbinsek and P. Günter, *J. Mater. Chem.*, 2006, **16**, 2839; (*b*) Z. Yang, M. Jazbinsek, B. Ruiz, S. Aravazhi, V. Gramlich and P. Günter, *Chem. Mater.*, 2007, **19**, 3512.

7 (*a*) H. Umezawa, K. Tsuji, S. Okada, H. Oikawa, H. Matsuda and H. Nakanishi, *Opt. Mater. (Amsterdam, Neth.)*, 2002, **21**, 75; (*b*) J. Ogawa, S. Okada, Z. Glavcheva and H. Nakanishi, *J. Cryst. Growth*, 2008, **310**, 836.

8 (*a*) B. J. Coe, J. A. Harris, I. Asselberghs, K. Clays, G. Olbrechts, A. Persoons, J. T. Hupp, R. C. Johnson, S. J. Coles, M. B. Hursthouse and K. Nakatani, *Adv. Funct. Mater.*, 2002, **12**, 110; (*b*) H. Figi, L. Mutter, Ch. Hunziker, M. Jazbinsek, P. Günter and B. J. Coe, *J. Opt. Soc. Am. B*, 2008, **25**, 1786; (*c*) B. J. Coe, J. A. Harris, I. Asselberghs, K. Wostyn, K. Clays, A. Persoons, B. S. Brunschwig, S. J. Coles, T. Gelbrich, M. E. Light, M. B. Hursthouse and K. Nakatani, *Adv. Funct. Mater.*, 2003, **13**, 347.

9 (*a*) G. L. Bryant, Jr, C. P. Yakymyshyn and K. R. Stewart, *Acta Crystallogr., Sect. C: Cryst. Struct. Commun.*, 1993, **49**, 350; (*b*) F. Pan, M. S. Wong, Ch. Bosshard and P. Günter, *Adv. Mater.*, 1996, **8**, 592; (*c*) D. C. Zhang, T. Z. Zhang, Y. Q. Zhang, Z. H. Fei and K. B. Yu, *Acta Crystallogr., Sect. C: Cryst. Struct. Commun.*, 1997, **53**, 364; (*d*) A. K. Bhowmik, J. Xu and M. Thakur, *Appl. Phys. Lett.*, 1999, **21**, 3291.

10 Ch. Bosshard, R. Spreiter and P. Günter, *J. Opt. Soc. Am. B*, 2001, **18**, 1620.

11 (*a*) S. R. Hammond, O. Clot, K. A. Firestone, D. H. Bale, D. Lao, M. Haller, G. D. Phelan, B. Carlson, A. K. Y. Jen, P. J. Reid and L. R. Dalton, *Chem. Mater.*, 2008, **20**, 3425; (*b*) I. Liakatas, C. Cai, M. Bösch, M. Jager, Ch. Bosshard, P. Günter, C. Zhang and L. R. Dalton, *Appl. Phys. Lett.*, 2000, **76**, 1368; (*c*) H. Ma, S. Liu, J. Luo, S. Suresh, L. Liu, S. H. Kang, M. Haller, T. Sassa, L. R. Dalton and A. K. Y. Jen, *Adv. Funct. Mater.*, 2002, **12**, 565.

12 (*a*) O. P. Kwon, B. Ruiz, A. Choubey, L. Mutter, A. Schneider, M. Jazbinsek, V. Gramlich and P. Günter, *Chem. Mater.*, 2006, **18**, 4049; (*b*) O. P. Kwon, S. J. Kwon, M. Jazbinsek, A. Choubey, V. Gramlich and P. Günter, *Adv. Funct. Mater.*, 2007, **17**, 1750; (*c*) L. T. Cheng, W. Tam, S. H. Stevenson, G. R. Meredith, G. Rikken and S. R. Marder, *J. Phys. Chem.*, 1991, **95**, 10631; (*d*) T. Tsunekawa, T. Gotoh and M. Iwamoto, *Chem. Phys. Lett.*, 1990, **166**, 353.

13 O. P. Kwon, M. Jazbinsek, J. I. Seo, E. Y. Choi, H. Yun, F. D. J. Brunner, P. Günter and Y. S. Lee, *J. Chem. Phys.*, 2009, **130**, 134708.

14 S. J. Kwon, O. P. Kwon, J. I. Seo, M. Jazbinsek, L. Mutter, V. Gramlich, Y. S. Lee, H. Yun and P. Günter, *J. Phys. Chem. C*, 2008, **112**, 7846.

15 (*a*) A. D. Becke, *J. Chem. Phys.*, 1993, **98**, 5648; (*b*) J. P. Perdew, *Phys. Rev. B: Condens. Matter Mater. Phys.*, 1986, **33**, 8822.

16 K. Kurtz and T. T. Perry, *J. Appl. Phys.*, 1968, **39**, 3798.

17 B. Ruiz, B. J. Coe, R. Gianotti, V. Gramlich, M. Jazbinsek and P. Günter, *CrystEngComm*, 2007, **9**, 772.

18 J. Y. Seo, S. B. Choi, M. Jazbinsek, F. Rotermund, P. Günter and O. P. Kwon, *Cryst. Growth Des.*, 2009, **9**, 5003.

19 G. M. Sheldrick, *Acta Crystallogr., Sect. A: Fundam. Crystallogr.*, 2008, **64**, 112.